

The improvement of the color rendering index using convex-dual-layer remote phosphor geometry with YOCl:Eu^{3+}

Dieu An Nguyen Thi¹, Binh Le Nguyen Hoa²

¹Faculty of Electrical Engineering Technology, Industrial University of Ho Chi Minh City, Ho Chi Minh City, Vietnam

²Faculty of Mechanical - Electrical and Computer Engineering, School of Engineering and Technology, Van Lang University, Ho Chi Minh City, Vietnam

Article Info

Article history:

Received Aug 28, 2021

Revised Oct 26, 2022

Accepted Nov 12, 2022

Keywords:

Color rendering index
Dual-layer remote phosphor geometry WLEDs
Mie-scattering theory
 YOCl:Eu^{3+}

ABSTRACT

White-light emitting diodes (WLEDs) are semiconductor light sources whose construction design is usually made up of a single pumping chip and a single light-conversion film of phosphor compound. The outstanding problem of this traditional setting is the inadequate chroma rendering index (CRI). Introducing a cluster of multiple blue chips with more than one phosphor layer is demonstrated to address that flaw of W-LEDs. This package is called the dual-film remote-phosphor multi-chip WLED. As a consequence, both the light brightness and the CRI are improved. However, for the maximum results, the test on the second layer of phosphor has been performed to continually alter the proportions and densities of phosphor within the silicone. The researchers employed a unique hue design to control the white-light light emitting diode (LED) module. When comparing the actual result to the simulated color coordinates under the hue standard of international commission on illumination (CIE) 1931, the highest difference is found to be around 0.0063 for correlated color temperatures (CCT) of 6600 K and 7700 K. Experiments indicate that the setting of multi-chip and dual-phosphorus is the optimal design for supporting CRI quality and luminous intensity.

This is an open access article under the [CC BY-SA](https://creativecommons.org/licenses/by-sa/4.0/) license.



Corresponding Author:

Binh Le Nguyen Hoa

Faculty of Mechanical - Electrical and Computer Engineering, School of Engineering and Technology
Van Lang University, Ho Chi Minh City, Vietnam

Email: binh.lnh@vlu.edu.vn

1. INTRODUCTION

Carbon nanostructures have improved significantly in recent decades in comparison to mass materials due to their better electrical, optical, and biocompatible properties. Fluorescent carbon dots (FCDs), in particular, are a popular issue among chemists, physicists, and materials scientists. In comparison to traditional heavy-metal quantum dots (QDs), including CdSe, CdTe, and PbS QDs, the FCDs feature distinctive fluorescence which makes them attractive alternatives for current fluorescent nanomaterials of diverse ecologically-friendly applications like low in toxic components, chemical resilience, and ease of fabrication [1]-[3]. The approaches established for FCD synthesis could be divided into two categories: bottom-up and top-down. In the bottom-up approach, the synthesizing procedure involves hydrothermal and microwave aided syntheses, as well as pyrolysis precursors. This approach uses small molecules and polymers, which are dehydrated and then carbonized, to manufacture FCDs. Along with cutting several types of carbon sources to manufacture carbon dots (CDs), the top-down process also consists of conventional laser ablation, electrochemical corrosion, and acid boiling. Unfortunately, inventing effective one-step solutions for large-scale CD synthesis is still a challenge in this sector [4]-[6]. As white-light emitting diodes (WLEDs) are widely believed

to become more essential for human life, the development of QDs-applied WLEDs will be constantly attractive. However, heavy metals such as cadmium, plumbum, and more, are still included in semiconductor QDs. These chemical components are extremely poisonous even with low concentrations, and thus can severely limit QD-WLEDs' practical uses [7]-[9]. Many researchers have recently discovered green synthesis techniques for synthesizing II-VI group QDs. These days, CD-based WLEDs are gaining popularity as an environmentally friendly option. The best thing we know is that the peaks of FCDs' emission are usually found to be centered in blue or blue-green wavelength regions, primarily at 440 nm under an illumination source of 340 nm – 380 nm. There were a few reports on [10]-[15] FCDs with photoluminescent (PL) variables that moved from blue to red. Yet, the insufficient quantum yields (QYs) in their performance were still outstanding. As a result, attaining the blue-emitting FCDs is regarded as one of the crucial priorities in the development of lighting devices that can address optical shortcomings such as limited color range and inadequate chroma rendering index (CRI). Furthermore, FCD-based WLEDs with YAG:Ce³⁺, or other yellow-emitting phosphor compositions, acting as a color conversion layer and excited by a ultraviolet (UV) chip, have been described, albeit their CRI values still need to be improved [16]-[18].

In this study, we offer an ammonium hydroxide modulated hydrothermal approach for producing high-performance FCDs with an appealing 40% QY by utilizing citric acid as the primary carbon source. We run a series of studies to see if the amino group has an effect on the strong fluorescent performance of the FCDs. Additionally, a model was developed to study fluorescence configuration. Meanwhile, WLEDs with an enhanced CRI have been created using the prepared FCDs and innovative rare earth luminous materials such as SrSi₂O₂N₂:Eu and Sr₂Si₅N₈:Eu. According to the findings, the high potential for environmentally friendly production and implementation of nontoxic FCDs geometry in WLEDs field is implied.

2. PREPARATION

The main phosphor we apply in this study is YOCl:Eu³⁺. Because of its rhombohedral (matlockite) structure, this phosphor is hygroscopic and must be stored in a dry environment. This phosphor's further optical features include a red emission hue, emission peaks ranging from 1.97 eV to 2.14 eV with the main one at 2.00 eV. Its excitation efficiencies by UV are ++ (4.88 eV) and – (3.40 eV), while by e-ray is negative [19]. The organization for YOCl:Eu³⁺ and YAG:Ce³⁺ film in constructing the required WLED configuration is depicted in Figure 1. Particularly, the phosphor layers are placed in the following order: silicone glues, YOCl:Eu³⁺ phosphor, and YAG:Ce³⁺ phosphor, see Figure 1(a). Figure 1(b) presents the essential parts of a WLED model, which include 9 blue chips divided into 3 parallel columns, 1 reflector cup, 2 convex phosphor films, and lastly silicone glue. The reflector that covers the chips has a depth of 2.07 mm, a bottom thickness of 8 mm, along with a length of 9.85 mm for the top exterior, as shown in Figure 1(c). At the peak wavelength measured at 453 nm, all nine blue chips emit equally a radiant intensity of 1.16 W, see Figure 1(d). For refractive index, YOCl:Eu³⁺ YAG:Ce³⁺ yield values measured at 1.85 and 1.83, respectively. The YAG:Ce³⁺ proportion must be adjusted in connection with the alteration for YOCl:Eu³⁺ proportion for balancing the YOCl:Eu³⁺ concentration and maintaining the average correlation chroma temperatures (ACCTs) that have been set for the studied model.

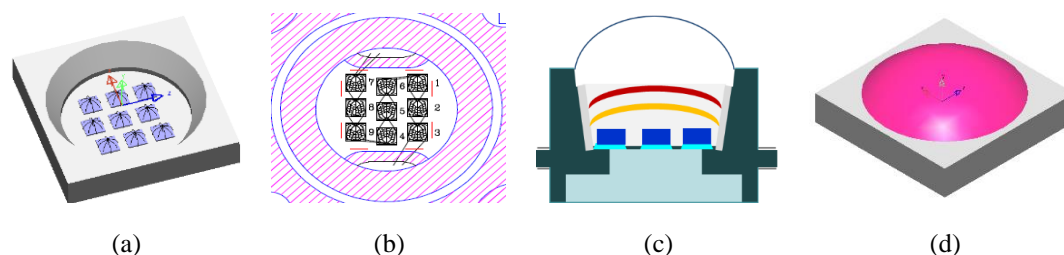


Figure 1. Graphical illustrations of WLED (a) 3D modeling for one multi-chip WLED, (b) binding graph of a multi-chip WLED, (c) cross-section model of pc-WLEDs with two convex phosphor-conversion layers, and (d) simulated WLEDs model by LightTools

Table 1. Composition table of YOCl:Eu³⁺

Ingredient	Mole %	By weight (g)
Y ₂ O ₃	95 (of Y)	107.4
Eu ₂ O ₃	5 (of Eu)	8.8
NH ₄ Cl	110	59

The compositions to create this substance will be exhibited by Table 1. The initial step is to dissolve all of the materials in water. The mixture must then be slowly heated to dryness, allowing the conversion of Y_2O_3 to $YOCl$ to occur. We powder the mixture after it has boiled down. After this step, there are two options. We can fire it in capped quartz tubes with N_2 for about $500\text{ }^\circ\text{C}$ for half an hour, or at $1100\text{ }^\circ\text{C}$ for 1 hour. After heating it up, we powder it once again and wash it in water several times. Finally, this mixture must be allowed to dry entirely. The study uses the software LightTools along with Mie hypothesis of scattering for generating the light emitting diode (LED) recreation and double-check the precision of the data [20], [21]. Following the details collected regarding the scattering characteristics of phosphor particles, which is supporting the study on the influence of phosphorus $YOCl:Eu^{3+}$ on WLEDs with a CCT measured at 5600 K, the task will be recreating WLEDs with double-layer phosphorus.

3. RESULTS AND DISCUSSION

Figure 2 depicts the fluctuation for the $YAG:Ce^{3+}$ proportion to maintain median ACCTs when $YOCl:Eu^{3+}$ percentage rises. Specifically, even though the weight percentage (wt%) of $YOCl:Eu^{3+}$ is increasing (2–26 wt%), $YAG:Ce^{3+}$ wt% apparently reduces to maintain ACCTs. This mechanism apply to WLED device under 5600 K. The variance based on these discoveries has an impact on scattering and absorption qualities, which could offer advancement to WLED luminescence in chroma strengths. As a result, selecting the concentration of $YOCl:Eu^{3+}$ phosphor is critical since it determines the performance of WLEDs.

Figure 3 shows the impact from $YOCl:Eu^{3+}$ concentrations at 2% and 24% on the light output intensity of the WLED with pre-set 5600 K ACCT. When introducing $YOCl:Eu^{3+}$ to the WLED structure, its white-light output is generated from three separate spectral wavelengths, including 420 nm – 480 nm, 500 nm – 640 nm, and the most prominent 648 nm – 738 nm. The line of red spectra rises, implying the higher red chroma power in the white light output, particularly benefiting the CRI performance. If the dispersed blue illumination is excited between the wavelengths of 420 nm and 480 nm, it will exhibit greater quality. The emission spectrum develops in proportion to the color temperature. In other words, the findings indicate the high probability to achieve white light with increasing CRI by using remote $YOCl:Eu^{3+}$ phosphor layer, which is efficient for a wide-range CCT, from low (6600 K) to high (7700 K) values. This discovery is critical since it guides manufacturers in choosing the appropriate concentration to make the optimal LEDs. On the other hand, as shown in previous studies, the luminous intensity (LI) of the increasing-CRI WLEDs may confront a minor drawback, which should be aware when being introduced to manufacturing.

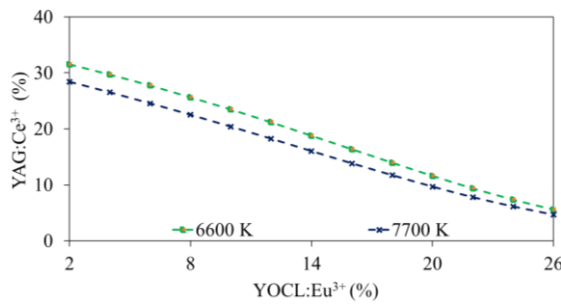


Figure 2. Mean CCT is sustained by the equilibrium among two phosphor contents

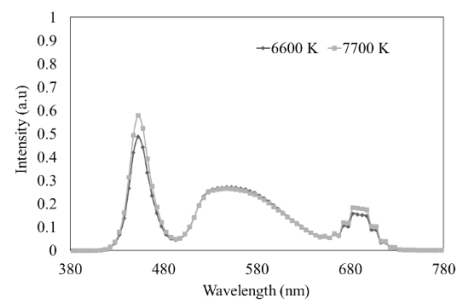


Figure 3. Intensities for WLED’s emission when adding $YOCl:Eu^{3+}$ layer

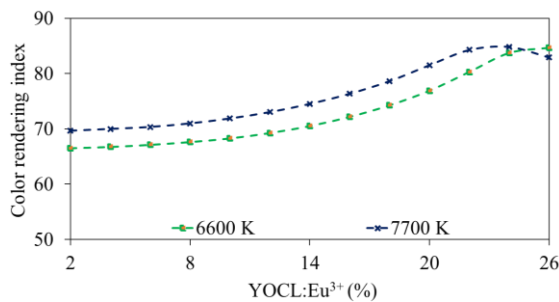


Figure 4. CRI corresponding to $YOCl:Eu^{3+}$ wt%

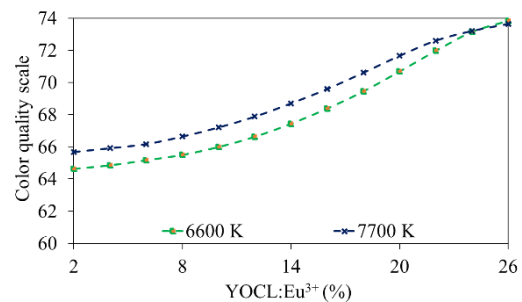


Figure 5. Color quality scale (CQS) corresponding to $YOCl:Eu^{3+}$ wt%

Because of red phosphor's ability to absorb light, the results of YOCL:Eu³⁺ in Figure 4 suggest that adding this phosphor can improve the color rendering index. YOCL:Eu³⁺ absorbs yellow light as well but the absorption feature is outstanding for the blue illumination, which would be ascribed to the phosphor's properties. Therefore, when the package comprises the phosphor YOCL:Eu³⁺, the red illumination, converted from absorbed blue rays, increases and benefits CRI efficiency. CRI is one of the most essential indications for determining a WLED's quality; higher the CRI performance often results in better WLED's color reproduction and thus may increase the manufacturing cost. As a result, because YOCL:Eu³⁺ phosphor is a low-cost approach, WLEDs with YOCL:Eu³⁺ may see further practical utilization. For not being a thorough indicator, CRI would not be considered vital when it comes to measuring hue output; instead, CQS would be viewed as one metric with better accuracy for conveying the performance of WLEDs. CQS has evolved into a hue output gauge with highest reliability, capable of examining particular characteristics of WLEDs: CRI efficiency, observers' visuality, and chromatic coordination. The effect of red phosphor YOCL:Eu³⁺ on improving the color adequacy as a function of CQS enhancement is presented in Figure 5. Despite its value in improving color-reproducing effectiveness, the factor that the output of light is reduced by increasing YOCL:Eu³⁺ wt% cannot be underestimated. The following section considers a hypothetical component that could improve LED efficiency and computational modules for transmitted and converted light components.

Gaussian function [22], [23] would be typically utilized for the task of representing the non-symmetrical spectrum power distribution (SPD) – P_λ (mW/nm) of a monochromatic LED:

$$P_\lambda = P_{opt} \frac{1}{\sigma\sqrt{2\pi}} \exp \left[-0.5 * \frac{(\lambda - \lambda_{peak})^2}{\sigma^2} \right] \quad (1)$$

$$\sigma = \frac{\lambda^2_{peak} \Delta E}{2hc\sqrt{2 \ln 2}} = \frac{\lambda^2_{peak} \left(\frac{hc}{\lambda_1} - \frac{hc}{\lambda_2} \right)}{2hc\sqrt{2 \ln 2}} = \frac{\lambda^2_{peak} \left(\frac{hc\Delta\lambda}{\lambda_1\lambda_2} \right)}{2hc\sqrt{2 \ln 2}} \quad (2)$$

Here, P_{opt} signifies illumination energy (W). λ_{peak} signifies the apex wavelength (nm). $\Delta\lambda$ is full-width at half-maximum (abbreviated as FWHM) (nm); σ is the $\Delta\lambda$ -related coefficient (nm) that depends on both λ_{peak} and $\Delta\lambda$; h and c are the Planck's constant (J.s) and the light speed ($m \cdot s^{-1}$), respectively. λ_1 , λ_2 present the wavelengths under 50% apex intensity.

P_λ of the WLED comprising YAG:Ce³⁺ yellow emitting phosphor and blue-emission chips can be demonstrated with the spectra combination of yellow and blue spectra. Both yellow and green spectra ranges are still present in lights emitted by the alleged yellow phosphor (as can be implied from the intentional spectra in Figure 3). If we pick one blue as well as one yellow zone, it is possible to use one green zone for the task of representing the difference among the fundamentally calculated SPD and the double hue (including blue along with yellow) zone setting. As a result, adding a green band to the double band module is required to make it a reality, revealing the following trispectrum model (blue, green, yellow), exhibited by (3) then modified by (4) [24], [25].

$$P_\lambda = P_{opt_b} \frac{1}{\sigma_b\sqrt{2\pi}} \exp \left[-0.5 * \frac{(\lambda - \lambda_{peak_b})^2}{\sigma_b^2} \right] + P_{opt_g} \frac{1}{\sigma_g\sqrt{2\pi}} \exp \left[-0.5 * \frac{(\lambda - \lambda_{peak_g})^2}{\sigma_g^2} \right] + P_{opt_y} \frac{1}{\sigma_y\sqrt{2\pi}} \exp \left[-0.5 * \frac{(\lambda - \lambda_{peak_y})^2}{\sigma_y^2} \right] \quad (3)$$

$$P_\lambda = \eta_b P_{opt_total} \frac{1}{\sigma_b\sqrt{2\pi}} \exp \left[-0.5 * \frac{(\lambda - \lambda_{peak_b})^2}{\sigma_b^2} \right] + \eta_g P_{opt_total} \frac{1}{\sigma_g\sqrt{2\pi}} \exp \left[-0.5 * \frac{(\lambda - \lambda_{peak_g})^2}{\sigma_g^2} \right] + \eta_y P_{opt_total} \frac{1}{\sigma_y\sqrt{2\pi}} \exp \left[-0.5 * \frac{(\lambda - \lambda_{peak_y})^2}{\sigma_y^2} \right] \quad (4)$$

Where η_b , η_g , η_y signify the ratio between the spectra (blue, green, yellow) and the white spectrum, respectively; P_{opt_b} , P_{opt_y} , P_{opt_g} , P_{opt_total} present the blue, yellow, green, and white spectral optical power, respectively; λ_{peak_b} , λ_{peak_y} , λ_{peak_g} are the peak spectral wavelengths of blue, yellow, and green. σ_b , σ_g , σ_y are $\Delta\lambda$ -related coefficients of the spectra (blue, green, yellow).

The dispersion for the YOCL:Eu³⁺ granules takes the Mie dispersion for simulation and investigation. Besides, when it comes to assessing the propagated illumination energy (I), the study applies the law of Lambert-Beer [26].

$$I = I_0 \exp(-\mu_{ext}L) \quad (5)$$

The incident illumination energy would be I_0 , the phosphor sheet breadth is L (mm), and the extinction coefficient (EC) is μ_{ext} which can be derived using (6).

$$\mu_{ext} = N_r \cdot C_{ext} \quad (6)$$

Where N_r expresses the density distribution of phosphor particles (mm^{-3}), and C_{ext} (mm^2) is the phosphor particle extinction cross-section.

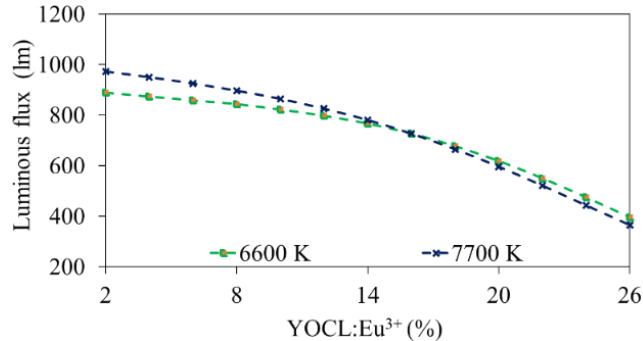


Figure 6. The LI of WLEDs corresponding to YOCL:Eu³⁺ wt%

The dual-layer remote phosphor configuration is demonstrated to produce notably more LI than the one-layered phosphor, implying from (5). As a result, the dual-layer phosphor design performs admirably and adds to the growth of WLED luminous flux. The concentration of red phosphor YOCL:Eu³⁺ substantially impacts the light qualities (chroma and luminous performances) of the dual-layer phosphor structure used in WLEDs. The EC μ_{ext} indicated by the Beer's law as well as the YOCL:Eu³⁺ content rise concurrently, but the illumination discharge power surges inversely to the EC. Consequently, increasing the phosphor layer thickness by adding more YOCL:Eu³⁺ lowers the light flux of WLEDs. Figure 6 supports this finding by displaying the declining LI following the increasing YOCL:Eu³⁺ concentration that goes up to 26 wt%. In general, compared to the single layer, more luminous flux is actually produced when the remote dual-film cluster of phosphors including red-emitting YOCL:Eu³⁺ is applied. Furthermore, YOCL:Eu³⁺ would yield provides significant boosts for CRI as well as CQS. Consequently, a modest penalty in luminous flux is reasonable given the benefits. Manufacturers choose the most appropriate YOCL:Eu³⁺ concentration setting in WLED mass production based on their quality requirements.

4. CONCLUSION

The study successfully employed a new module to develop and attain adequate CRI performance. This module is also introduced to perform a light-emitting WLED presenting the ability to change the target spectrum. A color model is constructed using the law of Lambert-Beer and linear conversion so that white light could be adjusted by LEDs to be aligned with the needs of the manufacturers. The simulated and measured spectrums are compatible; the highest variation is around 0.0063 at 5600 K CCT between the observed and international commission on illumination (CIE) 1931 simulations. The development and use of the model for chromatic design are aided by this feature.

ACKNOWLEDGEMENTS

This study was financially supported by Van Lang University, Vietnam.




REFERENCES

- [1] B. Zhang *et al.*, "Rapid, large-scale stimulated Raman histology with strip mosaicing and dual-phase detection," *Biomedical Optics Express*, vol. 9, no. 6, pp. 2604-2613, 2018, doi: 10.1364/BOE.9.002604.
- [2] A. Ahmad, A. Kumar, V. Dubey, A. Butola, B. S. Ahluwalia, and D. S. Mehta, "Characterization of color cross-talk of CCD detectors and its influence in multispectral quantitative phase imaging," *Optics Express*, vol. 27, no. 4, pp. 4572-4589, 2019, doi: 10.1364/OE.27.004572.
- [3] C. J. C. Smyth, S. Mirkhanov, A. H. Quarterman, and K. G. Wilcox, "27.5 W/m² collection efficiency solar laser using a diffuse scattering cooling liquid: erratum," *Applied Optics*, vol. 59, no. 3, 2020, doi: 10.1364/AO.386409.
- [4] T. P. White, E. Deleporte, and T. -C. Sum, "Feature issue introduction: halide perovskites for optoelectronics," *Optics Express*, vol. 26, no. 2, pp. A153-A156, 2018, doi: 10.1364/OE.26.00A153.
- [5] V. B. -Yekta and T. Tiedje, "Limiting efficiency of indoor silicon photovoltaic devices," *Optics Express*, vol. 26, no. 22, pp. 28238-28248, 2018, doi: 10.1364/OE.26.028238.
- [6] Q. Xu, L. Meng, and X. Wang, "Nanocrystal-filled polymer for improving angular color uniformity of phosphor-converted white LEDs," *Applied Optics*, vol. 58, no. 27, pp. 7649-7654, 2019, doi: 10.1364/AO.58.007649.




- [7] Z. Wen *et al.*, "Fabrication and optical properties of Pr³⁺-doped Ba, (Sn, Zr, Mg, Ta) O₃ transparent ceramic phosphor," *Optics Letters*, vol. 43, no. 11, pp. 2438-2441, 2018, doi: 10.1364/OL.43.002438.
- [8] C. Zhang, L. Xiao, P. Zhong, and G. He, "Photometric optimization and comparison of hybrid white LEDs for mesopic road lighting," *Applied Optics*, vol. 57, no. 16, pp. 4665-4671, 2018, doi: 10.1364/AO.57.004665.
- [9] J. Li, Y. Tang, Z. Li, X. Ding, L. Rao, and B. Yu, "Investigation of stability and optical performance of quantum-dot-based LEDs with methyl-terminated-PDMS-based liquid-type packaging structure," *Optics Letters*, vol. 44, no. 1, pp. 90-93, 2019, doi: 10.1364/OL.44.000090.
- [10] S. An, J. Zhang, and L. Zhao, "Optical thermometry based on upconversion luminescence of Yb³⁺-Er³⁺ and Yb³⁺-Ho³⁺ doped Y₆WO₁₂ phosphors," *Applied Optics*, vol. 58, no. 27, pp. 7451-7457, 2019, doi: 10.1364/AO.58.007451.
- [11] D. Molter, M. Kolano, and G. V. Freymann, "Terahertz cross-correlation spectroscopy driven by incoherent light from a superluminescent diode," *Optics Express*, vol. 27, no. 9, pp. 12659-12665, 2019, doi: 10.1364/OE.27.012659.
- [12] S. Cincotta, C. He, A. Neild, and J. Armstrong, "High angular resolution visible light positioning using a quadrant photodiode angular diversity aperture receiver (QADA)," *Optics Express*, vol. 26, no. 7, pp. 9230-9242, 2018, doi: 10.1364/OE.26.009230.
- [13] L. V. Labunets, A. B. Borzov, and I. M. Akhmetov, "Regularized parametric model of the angular distribution of the brightness factor of a rough surface," *Journal of Optical Technology*, vol. 86, no. 10, pp. 618-626, 2019, doi: 10.1364/JOT.86.000618.
- [14] T. DeLawyer, M. Tayon, C. -L. Yu, and S. L. Buck, "Contrast-dependent red-green balance shifts depend on S-cone activity," *Journal of the Optical Society of America A*, vol. 35, no. 4, pp. B114-B121, 2018, doi: 10.1364/JOSAA.35.00B114.
- [15] Z. Li, J. Zheng, J. Li, W. Zhan, and Y. Tang, "Efficiency enhancement of quantum dot-phosphor hybrid white-light-emitting diodes using a centrifugation-based quasi-horizontal separation structure," *Optics Express*, vol. 28, no. 9, pp. 13279-13289, 2020, doi: 10.1364/OE.392900.
- [16] T. Shao *et al.*, "Understanding the role of fluorine-containing plasma on optical properties of fused silica optics during the combined process of RIE and DCE," *Optics Express*, vol. 27, no. 16, pp. 23307-23320, 2019, doi: 10.1364/OE.27.023307.
- [17] Y. Tian *et al.*, "Study of composite Al₂O₃-Ce:Y₃Mg_{1.8}Al_{1.4}Si_{1.8}O₁₂ ceramic phosphors," *Optics Letters*, vol. 44, no. 19, pp. 4845-4848, 2019, doi: 10.1364/OL.44.004845.
- [18] A. Keller, P. Bialecki, T. J. Wilhelm, and M. K. Vetter, "Diffuse reflectance spectroscopy of human liver tumor specimens - towards a tissue differentiating optical biopsy needle using light emitting diodes," *Biomedical Optics Express*, vol. 9, no. 3, pp. 1069-1081, 2018, doi: 10.1364/BOE.9.001069.
- [19] C. -H. Lin *et al.*, "Hybrid-type white LEDs based on inorganic halide perovskite QDs: candidates for wide color gamut display backlights," *Photonics Research*, vol. 7, no. 5, pp. 579-585, 2019, doi: 10.1364/PRJ.7.000579.
- [20] Y. -P. Chang *et al.*, "An advanced laser headlight module employing highly reliable glass phosphor," *Optics Express*, vol. 27, no. 3, pp. 1808-1815, 2019, doi: 10.1364/OE.27.001808.
- [21] Y. -C. Jen *et al.*, "Design of an energy-efficient marine signal light based on white LEDs," *OSA Continuum*, vol. 2, no. 8, pp. 2460-2469, 2019, doi: 10.1364/OSAC.2.002460.
- [22] X. Ding *et al.*, "Improving the optical performance of multi-chip LEDs by using patterned phosphor configurations," *Optics Express*, vol. 26, no. 6, pp. A283-A292, 2018, doi: 10.1364/OE.26.00A283.
- [23] Y. Sun, Y. Yang, H. Ma, and Y. Sun, "Improving the Color Gamut of a Liquid-crystal Display by Using a Bandpass Filter," *Current Optics and Photonics*, vol. 3, no. 6, pp. 590-596, 2019. [Online]. Available: https://opg.optica.org/DirectPDFAccess/2C1A84FE-5977-4659-ADE5FEA3A97715EC_425527/copp-3-6-590.pdf?da=1&id=425527&seq=0&mobile=no
- [24] J. Hao, H. -L. Ke, L. Jing, Q. Sun, and R. -T. Sun, "Prediction of lifetime by lumen degradation and color shift for LED lamps, in a non-accelerated reliability test over 20,000 h," *Applied Optics*, vol. 58, no. 7, pp. 1855-1861, 2019, doi: 10.1364/AO.58.001855.
- [25] R. Deeb, J. V. D. Weijer, D. Muselet, M. Hebert, and A. Treneau, "Deep spectral reflectance and illuminant estimation from self-interreflections," *Journal of the Optical Society of America A*, vol. 36, pp. 105-114, 2019, doi: 10.48550/arXiv.1812.03559.
- [26] M. Hu, *et al.*, "Broadband emission of double perovskite Cs₂Na_{0.4}Ag_{0.6}In_{0.995}Bi_{0.005}Cl₆:Mn²⁺ for single-phosphor white-light-emitting diodes," *Optics Letters*, vol. 44, no. 19, pp. 4757-4760, 2019, doi: 10.1364/OL.44.004757.

BIOGRAPHIES OF AUTHORS



Dieu An Nguyen Thi    received a master of Electrical Engineering, HCMC University of Technology and Education, VietNam. Currently, she is a lecturer at the Faculty of Electrical Engineering Technology, Industrial University of Ho Chi Minh City, Viet Nam. Her research interests are Theoretical Physics and Mathematical Physics. She can be contacted at email: nguyenthidieuan@iuh.edu.vn.



Binh Le Nguyen Hoa    received the ME degree in Energy Economic and Planning from Asian Institute of Technology (AIT), Thailand, he is working as a lecturer at the Faculty of Mechanical - Electrical and Computer Engineering, School of Engineering and Technology, Van Lang University, Ho Chi Minh City, Vietnam. His research interests involve renewable energy, solar energy, power electric, control and automation in factory. He can be contacted at email: binh.lnh@vlu.edu.vn.